JACS
JOURNAL OF THE AMERICAN CHEMICAL SOCIETY

Article

pubs.acs.org/JACS

Dynamics of Excitation Energy Transfer Between the Subunits of Photosystem II Dimer

Yusuke Yoneda,[†] Tetsuro Katayama,[†] Yutaka Nagasawa,*[,†,‡,§] Hiroshi Miyasaka,[†] and Yasufumi Umena[∥]

[†]Graduate School of Engineering Science, Osaka University, Toyonaka, Osaka560-8531, Japan
[‡]College of Life Science, Ritsumeikan University, Kusatsu, Shiga 525-8577, Japan
[§]PRESTO, Japan Science and Technology Agency (JST), Kawaguchi, Saitama 332-0012, Japan
[∥]Research Institute for Interdisciplinary Science, Okayama University, Kita-ku, Okayama 700-8530, Japan

Supporting Information

ABSTRACT: Energy transfer dynamics in monomer and dimer of the photosystem II core complex (PSII-CC) was investigated by means of femtosecond transient absorption (TA) spectroscopy. There is no profound difference between the TA dynamics of the monomer and the dimer in the weak excitation intensity condition (≤21 nJ). However, the fast recovery of the ground state bleach was pronounced at higher excitation intensities, and the excitation intensity dependence of the dimer was more significant than that of the monomer. This result indicates efficient exciton−exciton annihilation taking place in the dimer due to energy transfer between the two monomer units. The annihilation dynamics was reproduced by a simple model based on binomial theorem, which indicated that although PSII-CC dimer has two reaction centers, only one charge-separated state remained after annihilation.

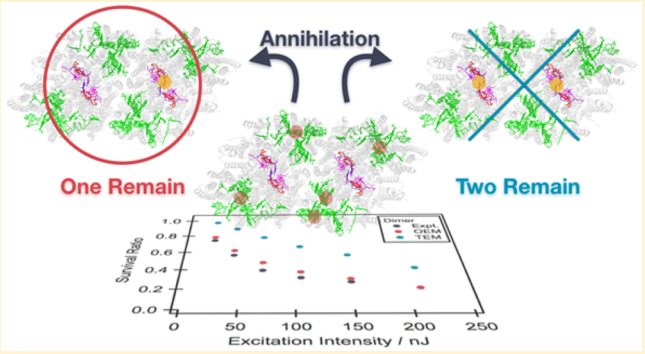

INTRODUCTION

Photosystem II core complex (PSII-CC) of higher plants and cyanobacteria plays a crucial role in primary processes in photosynthetic reactions, i.e., harvesting solar energy, triggering charge transfer, and oxidizing water.[1,2] Unveiling the precise structure[3−7] and dynamics[8−17] of PSII-CC has been attracting much attention toward understanding the mechanism of the excellent photofunction. PSII-CC consists of two antenna polypeptides (AP), CP43 and CP47, which contain 13 and 16 antenna chlorophyll *a* (Chl) molecules, respectively, and the D1/D2-cyt$_{b559}$ reaction center (RC) polypeptides.

A number of time-resolved spectroscopic studies have been applied, and kinetic models of energy and electron transfer in PSII-CC were developed. One such major model assumes that the excited state reaches an energy equilibration in a few picoseconds among the Chls in the antenna and also in the RC polypeptides, i.e., the "exciton/radical pair equilibrium (ERPE) model".[8,9] An alternative model assumes that the overall charge separation (CS) is severely limited by the energy transfer to the RC, i.e., the "transfer-to-the-trap limited (TTTL) model".[10,11] The crystallographic structure of PSII-CC revealed that the distance of the antenna Chls to the RC pigments is ∼25 Å,[7] which seems to be in favor of the TTTL model. However, to the best of our knowledge, the mechanism is still under discussion.[12,13]

PSII-CC in cyanobacteria is generally considered to exist in a dimeric form,[18−20] although some researchers emphasize that the formation of PSII-CC dimer is caused by the artificial purification process.[21,22] The numbers and the arrangements of chromophores are essentially the same in monomer and dimer,[23] and the ground state absorption spectra of monomer and dimer are nearly identical, indicating only a weak interaction between the two monomers in a dimer. Nevertheless, energy transfer is expected between the subunits of the dimer because some of the distances between Chls are sufficiently short, i.e., Chl27-Chl27 is 29 Å and Chl$_{ZD1}$-Chl29 is 31 Å (Chl numbering according to the nomenclature of Loll et al.[5]). Recently, Shibata et al. reported a simulation based on dimeric structure, and they predicted that energy transfer from Chl29 to Chl$_{ZD1}^{+}$ could take place with a time constant of 75 ps.[14]

Although the numerical simulation suggests energy transfer between the subunits in the dimer, the difference in the function and the advantage of the dimer has not yet been clarified.[24] In the present work, we have applied femtosecond transient absorption (TA) measurements at room temperature for highly purified PSII-CC monomer and dimer (details are shown in MATERIALS AND METHODS). The excitation

Received: April 27, 2016
Published: August 19, 2016

DOI: 10.1021/jacs.6b04316
J. Am. Chem. Soc. 2016, 138, 11599−11605

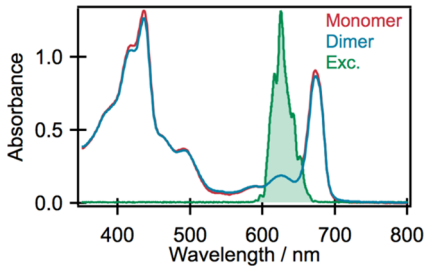

Figure 1. (a) Steady-state absorption spectra of PSII-CC monomer (red curve) and dimer (blue curve). The spectrum of laser pulse used in the TA experiment is also shown (green curve).

intensity dependence was compared and analyzed by a simple model based on binomial theorem.

RESULTS AND DISCUSSION

Steady-State Absorption Spectra. The steady-state absorption spectra of PSII-CC monomer and dimer (Figure 1) consist of $S_2 \leftarrow S_0$ transition band of β-caroten at 380−525 nm[25] and Soret band and Q_y band of Chl *a* at 380−460 nm and at 560−700 nm, respectively.[26] There is no significant difference between the ground state absorption spectra of monomer and dimer. This indicates that there is no strong interaction between the two monomers in a dimer.

For selective excitation of the blue-absorbing portion of the antenna Chls and avoiding direct excitation of the special pair in the RC, we have used an excitation laser pulse centered at 640 nm (20 fs pulse duration, Figure 1). This excitation wavelength is 830 cm^{-1} higher than the ground state absorption maximum of PSII-CC at 676 nm, although contribution from vibrational cooling was unobservable and the dynamics were nearly identical with the previous reports, as will be discussed in the following section.

Dynamics in Weak Excitation Intensity. Portion of the obtained ultrafast TA spectra of PSII-CC monomer in weak excitation intensity condition (21 nJ, which corresponds to fluence of 1.0×10^{14} photons $pulse^{-1}$ cm^{-2}; see Supporting Information for details) are shown in Figure 2a. Immediately after the photoexcitation, the negative signal, which is attributed to the ground state bleach (GSB) of the Q_y band of Chl, was observed in the wavelength range of 650−700 nm. The shoulder at 670 nm can be assigned to a Chl in CP43 or peripheral Chl_Z,[12,25,27−29] which disappeared in a few picosecond, and simultaneously, the minimum at 680 nm deepened. This indicates that energy equilibrium between blue and red absorbing Chls occurs in an ultrafast time range. One can notice an isosbestic point at 676 nm within 1 ps time range. Figure 2b shows time traces of transient absorbance of PSII-CC monomer. The signal at 670 nm can be reproduced by double exponential decay with time constants (relative amplitude) of 130 ± 10 fs (0.75) and 1.0 ± 0.1 ps (0.25), and the signal at 680 nm can be reproduced by 170 ± 10 fs rise. These results are consistent with previous lifetime density analysis.[12] The faster components (100−200 fs) are assigned to energy transfer within the antenna complexes CP43 and CP47,[12,27] and the slower component (1.0 ps) is attributable to antenna/RC equilibration.[12]

The TA dynamics for longer time region is shown in Figure 3. The deepening of the minimum at 540 nm (bleaching of a pheophytin ground state Q_x absorption band[15]) and the rise of the maximum at 460 nm (pheophytin anion absorption band[15])

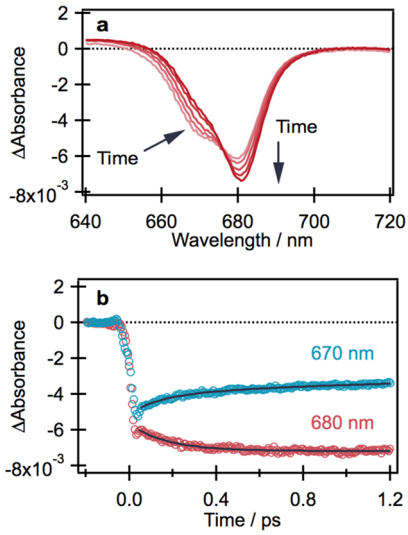

Figure 2. (a) TA spectra of PSII-CC monomer at 50, 100, 200, 500, and 1000 fs in the wavelength range of 640−720 nm, which corresponds to the GSB of the Q_y band of Chl. (b) Time traces of the transient absorbance of PSII-CC monomer at 670 nm (blue circle) and 680 nm (red circle). Black curves show fitting results.

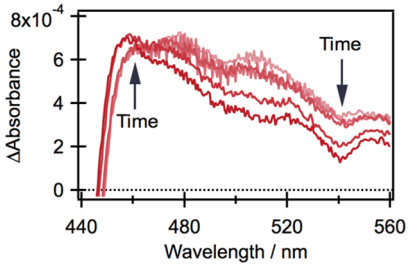

Figure 3. TA spectra of PSII-CC monomer at 1, 5, 10, 50, and 100 ps in the wavelength range of 440−560 nm.

occurred simultaneously within 100 ps, indicating the formation of the CS state in RC, which is consistent with previously reported time scales of 35 to 60−80 ps.[8,30]

The TA spectra of the dimer (Figures S1 and S2) exhibit almost the same results as those of the monomer, indicating that there is no significant difference between the dynamics of the monomer and the dimer in the weak excitation intensity condition as expected from the steady-state spectra.

Excitation Intensity Dependence. On the other hand, a significant difference was observed under the condition with higher excitation intensity. Figure 4 shows time traces of differential absorbances of PSII-CC monomer and dimer probed at 676 nm for various excitation intensities. The wavelength of 676 nm overlaps with the isosbestic point in the ultrafast time region (Figure 1b); thus, the results are free from the effect of ultrafast energy equilibration. With increasing excitation intensities, fast recovery of the GSB signal was pronounced, of which results are attributed to exciton−exciton annihilation. Generally, annihilation is observed for antenna complexes such as light-harvesting complex 2 (LH2) in high-intensity pulse laser conditions.[31,32] Although no significant difference was observed between the monomer and the dimer in the weak excitation intensity conditions, the rapid recovery of GSB is more clearly observed at higher intensities for the dimer, indicating that energy transfer between the subunits is present in the dimer.

DOI: 10.1021/jacs.6b04316
J. Am. Chem. Soc. 2016, 138, 11599−11605

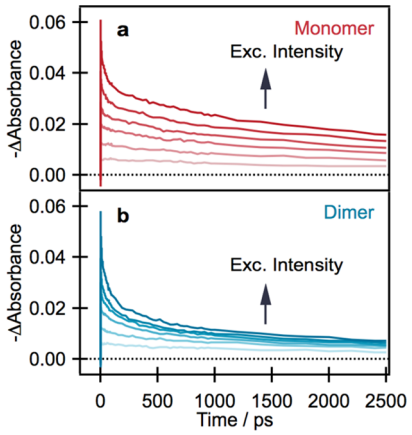

Figure 4. Time traces of differential absorbance of PSII-CC (a) monomer and (b) dimer obtained by probing at 676 nm for various excitation intensities of 21, 42, 70, 105, 150, and 210 nJ.

A monomer PSII-CC contains two APs, CP43 and CP47, each of which consists of Chl domains. Thus, annihilation time scales are expected to be different between inter- and intra-AP annihilation. However, the spectrum of PSII-CC is a superposition of all the Chls included in the complex, and the individual process is hardly separable from the ensemble-averaged dynamics. For such reasons, we assumed that (a) the number of decay components and (b) the time constants associated with annihilation depend on excitation intensity and the number of Chls in a single particle, i.e., monomer or dimer PSII-CC. On the other hand, normalized TA spectra at 2 ns are superimposable, indicating that the final product does not depend on excitation intensity (Figure S5). Thus, we assumed that TA signal of the PSII-CC monomer at 676 nm in the weakest excitation intensity condition decays single exponentially with a time constant of >2000 ps, and this component is independent of excitation intensity. In other words, additional decay components observed in higher excitation intensity conditions are solely due to exciton−exciton annihilation. On the basis of the above assumptions, we analyzed the excitation intensity-dependent TA signals by adding faster decay components to a single exponential function with its time constant fixed to >2000 ps

$$\Delta A_{676}(t) = A_0 \exp(-t/\tau_0) + \sum_{i\geq 1} A_i \exp(-t/\tau_i) \quad (1)$$

with τ_0 > 2000 ps. The number of additional components was increased while the relative amplitude of the added component was larger than 10%.

The results obtained by the analysis using eq 1 are summarized in Table 1. With increasing excitation intensity, the number of decay components increased, and the relative amplitude of the nanosecond component decreased. These trends are due to the increased number of excitons created in a single particle by larger excitation intensity. For the PSII-CC monomer, a component with time constant of 65−110 ps can be observed when the excitation intensity is larger than 70 nJ. With a further increase of intensity, a component with time constant of 5−8 ps appears in the range of >150 nJ. For the PSII-CC dimer, a 130−250 ps component was observed for all intensities, whereas a 5−8 ps component was only observable in the range of >70 nJ.

Annihilation in the monomer can be divided into two categories: "annihilation in the same AP" and "annihilation between different APs". Raszewski and Renger reported that energy transfer from one Chl domain to another Chl domain in the same AP proceeds in 0.7−7 ps between 80% of Chls.[13] Therefore, the time constant of 5−8 ps observed in both PSII-CC monomer and dimer is in the time scale of intra-AP annihilation. On the other hand, energy transfer from Chls in AP to RC is estimated to be $\tau_{AP\text{-}RC}$ = 20−40 ps.[13] Encounter of two excitons generated in different APs (CP43 and CP47) in a monomer PSII-CC requires one of them to cross over the RC and reach the other AP. Thus, inter-AP annihilation might require more than twice the time than the energy transfer from the AP to RC. Therefore, a time constant of 65−110 ps in the PSII-CC monomer, somewhat longer than that of $2\tau_{AP\text{-}RC}$, is close to the time scale of inter-AP annihilation. In a dimer, "annihilation between the two monomers" can also occur in addition to the above cases. As mentioned earlier, energy transfer from Chl29 to Chl_{ZD1}^{+} could take place with a time constant of τ_{interM} = 75 ps.[14] The time constant of energy transfer between Chl29 and other Chl domain in CP47 is τ_{Chl29} = 10−45 ps. Overall time is estimated to be $\tau_{interM} + \tau_{Chl29}$ (+ $2\tau_{AP\text{-}RC}$) = 85−120 (125−200) ps. Thus, time constant of 130−250 ps observed in the PSII-CC dimer could be partly related to intermonomer annihilation. In the dimer, because the time constants are in the same time scale, contribution of inter-AP annihilation could not be separated from the intermonomer annihilation.

Table 1. Time Constants (τ_{0-2}/ps) and Relative Amplitude (A_{0-2}) Obtained by Regression Analysis of the Time Traces of Differential Absorbance at 676 nm for PSII-CC Monomer and Dimer at Various Excitation Intensities

	intensity [nJ]	21	42	70	105	150	210
monomer	A_0	1.00	1.00	0.84	0.77	0.62	0.52
	τ_0	>2000	>2000	>2000	>2000	>2000	>2000
	A_1			0.16	0.23	0.20	0.26
	τ_1			100 ± 10	65 ± 5	110 ± 10	78 ± 4
	A_2					0.18	0.21
	τ_2					6.5 ± 0.6	4.8 ± 0.3
dimer	A_0	0.87	0.70	0.48	0.41	0.35	0.29
	τ_0	>2000	>2000	>2000	>2000	>2000	>2000
	A_1	0.13	0.30	0.39	0.39	0.39	0.41
	τ_1	240 ± 70	130 ± 10	250 ± 10	210 ± 10	160 ± 10	130 ± 10
	A_2			0.13	0.20	0.26	0.30
	τ_2			6.8 ± 0.6	7.4 ± 0.4	7.6 ± 0.5	7.2 ± 0.5

DOI: 10.1021/jacs.6b04316
J. Am. Chem. Soc. 2016, 138, 11599−11605

The inter-AP annihilation time scale seems to be comparable to the energy equilibrium time scale of 1−2 ps, suggesting annihilation might affect the energy equilibrium dynamics. Thus, we have compared the normalized TA spectra at 1 ps (Figure S4). However, no significant change was observed. This indicates that the energy equilibrium process is fast enough not to be affected by the annihilation process.

Annihilation Modeling. For quantitative analysis of exciton−exciton annihilation, we have estimated the decrement of excitons by annihilation from experimental data and also by calculations. We defined the survival ratio of excitons, S_{Ratio}, as the number of excitons after the annihilation divided by that of the initially excited ones (Figure 5). A smaller value of the S_{Ratio} indicates that excitons are more effectively quenched by the annihilation.

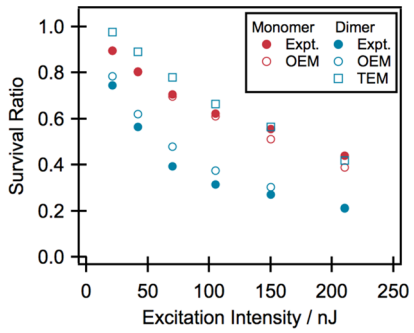

Figure 5. Calculated (red and blue open circles and squares) and experimentally obtained (red and blue closed circles) survival ratio of Chl excitons.

The simplest way to estimate the survival ratio is to divide the value of the differential absorbance at 676 nm after 2 ns, $\Delta A_{676}(2\ \text{ns})$, by that at the time origin, $\Delta A_{676}(0\ \text{fs})$, i.e., $S_{Ratio} \sim \Delta A_{676}(0\ \text{fs})/\Delta A_{676}(2\ \text{ns})$. However, other relaxation processes such as charge separation (CS) and emission decay take place, which compete with annihilation. Thus, the value of S_{Ratio} is obtained as

$$S_{Ratio} = \frac{\Delta A_{676}(2\ \text{ns})}{\Delta A_{676}(0\ \text{fs})} \Big/ \frac{\Delta A_{676}(2\ \text{ns})^*}{\Delta A_{676}(0\ \text{fs})^*} \tag{2}$$

where $\Delta A(t)^*$ indicates the value of differential absorbance without the effect of annihilation, and the term $\Delta A_{676}(2\ \text{ns})^*/\Delta A_{676}(0\ \text{fs})^*$ compensates the decrement caused by other competing relaxation processes. In this study, it was obtained by calculating the value for the monomer in the weakest excitation intensity condition based on the method described below. The results obtained by eq 2 are depicted in Figure 5 as closed circles.

The survival ratio of excitons, S_{Ratio}, was also calculated based on binomial theorem. First, the initial ratio of excited Chls against all the Chls, a, can be estimated from the initial amplitude of transient absorbance at 676 nm at time origin, ΔA_{676} (0 fs), and the ground state absorbance, A_{676},

$$a = -\frac{\Delta A_{676}(0\ \text{fs})}{A_{676}} \tag{3}$$

The value of a is plotted against excitation intensity in Figure S6 as closed circles, which exhibits a linear intensity dependence. The initial ratios of monomer and dimer are almost the same because they depend on the molar extinction coefficient of Chl and excitation intensity but not on the number of Chls in a single PSII-CC particle (the value of a can also be estimated by fluence and cross section; details are discussed in the Supporting Information).

Second, the probability for the production of j-excitons in a single PSII-CC particle, P_j $(0 \le j \le n)$, can be estimated by binomial theorem

$$P_j = {}_nC_j a^j (1-a)^{n-j} \tag{4}$$

where ${}_nC_j$ is the number of j-combinations of an n-element set, n is the number of Chls in a single particle (n = 35 for the monomer and n = 70 for the dimer), and a portion of P_j at various excitation intensities are shown in Figure 6 (details are shown in Figure S7). The probabilities of more than one exciton in a single PSII-CC particle are larger for the dimer than for the monomer at the same excitation intensities.

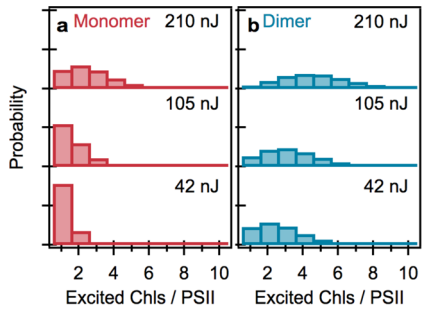

Figure 6. Probability for the production of j-excitons in a single PSII-CC monomer (a) and dimer (b) particle at different excitation intensities.

If excitons in a single PSII-CC particle decrease to one exciton by annihilation (one exciton model (OEM), Scheme 1a), the ratio of remaining excitons can be expressed as

$$S_{Ratio} = \frac{\sum_{j\ge 1} P_j}{\sum_j jP_j} \tag{5}$$

The remaining single exciton induces CS in the RC; thus, S_{Ratio} is also the ratio of produced charge-separated state against the number of initial excitons. The results obtained by eq 5 are plotted in Figure 3 as open circles.

In the case of the PSII-CC dimer, it should be considered that two CS states can be produced from two remaining excitons because a dimer contains two RCs (two excitons model (TEM), Scheme 1b). In this case, the ratio of the two remaining excitons against the initial ones can be expressed as

$$S_{Ratio} = \frac{P_1 + \sum_{j\ge 2} 2P_j}{\sum_j jP_j} \tag{6}$$

The results obtained by eq 6 are depicted in Figure 3 as open squares.

For the PSII-CC monomer, OEM reproduces the experimental results significantly well. The time constants of annihilations vary from 5 to 8 ps to 65−110 ps. In the previous report, the time constant of initial-CS and irreversible-CS were estimated to be 5.9−11[13,33] and 300−560 ps,[33,34] respectively. Some portion of fluorescence can be observed until irreversible-CS,[10,35] and annihilation can take place. In the monomer, annihilation time constants are faster than irreversible-CS, suggesting the relationship between the time

DOI: 10.1021/jacs.6b04316
J. Am. Chem. Soc. 2016, 138, 11599−11605

Scheme 1. Annihilation Models of PSII-CC for (a) OEM and (b) TEM[a]

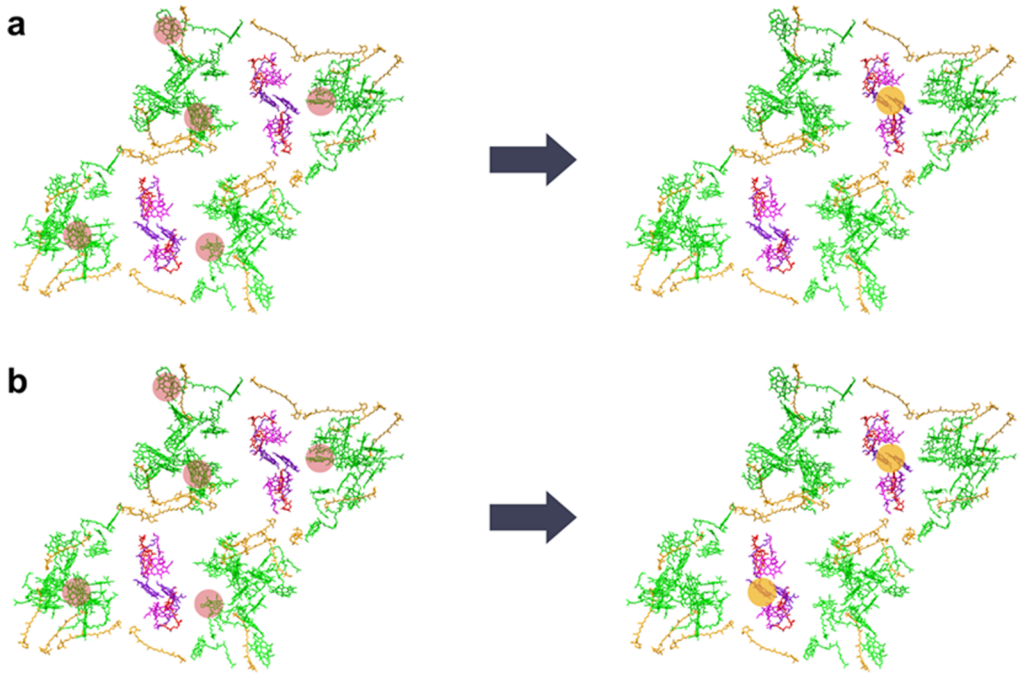

[a]Cofactor arrangements in PSII-CC shown as a view from the stromal side. One monomer unit contains 35 Chls (green), including special pair (purple) and accessory Chls (pink), 11 β-carotenes (orange), and 2 pheophytins (red). The arrangement was depicted from the crystallographic structure of PSII-CC from *Thermosynechococcus vulcanus*: 3WU2.[3] Red circles show exciton state, and yellow circles show CS state. Left side shows immediately after the photoexcitation, and right side shows after annihilation.

scales of annihilation and irreversible-CS is consistent with the result of S_{Ratio}.

For the dimer, further consideration will be needed. The time scale of annihilations in the dimer vary from 5 to 8 ps to 130−250 ps. The time constant of intermonomer annihilation, 130−250 ps, seems to be slower than dominant fluorescence lifetime decay of 60−80 ps.[8] This indicates that initial-CS can occur, and the exciton might be trapped by RC before intermonomer energy transfer. Hence, it can be expected that the S_{Ratio} of the dimer should be located between OEM and TEM. However, the present experimental results clearly show OEM reproduces experimental results better than that of TEM. This indicates that only one CS state remained after annihilation, although the PSII-CC dimer has two RCs. As mentioned previously, long-lived components (>100 ps) were observed in the previous fluorescence lifetime experiment, which were assigned to charge recombination.[35] This suggests that the CS state can go back to the exciton state until irreversible-CS. The back electron transfer rate of initial RP to RC* is estimated to be 25−32 ps.[12,34] Although the initial-CS process and secondary radical pair formation are also fast at 5.9−11[33,34] and 7.7−8.9 ps,[12,34] these time constants are much faster than irreversible-CS of 300−560 ps,[33,34] which suggests the exciton state and CS state reach equilibrium prior to the irreversible CS. Furthermore, Raszewski and Renger reported that disorder-averaged excitation energy transfer from RC to AP (16−22 ps) is faster than that from AP to RC (41−50 ps).[13] Thus, we concluded that the CS state can go back to the exciton state to some extent and run away from RC until irreversible-CS, which leads to annihilation for a longer time.

Recently, Chmeliov et al. performed a simple conceptual model describing excitation diffusion in a continuous medium and concluded that the multiexponential fluorescence decay of the PSII supercomplexes originates from the inhomogeneous distribution of connectivity between pigment−protein complexes.[36] For PSII dimer, wide distribution of the intersubunit energy transfer rate could also contribute to slower annihilation and lead to an exciton survival ratio between one and two; however, our experimental result suggested a one exciton model.

CONCLUSIONS

We have compared the primary dynamics of PSII-CC monomer and dimer at room temperature and obtained evidence of energy transfer between the subunits within the dimer. The annihilations were divided into three processes, and the time constant for each process was estimated to be (i) 5−8 ps for "intra-AP annihilation", (ii) 65−100 ps for "inter-AP annihilation", and (iii) 130−250 ps for "intermonomer annihilation". The exciton−exciton annihilation dynamics was analyzed based on binomial theorem, and it was concluded that, even in the dimer, only a single exciton remains to produce a CS state. This result suggests that CS state and exciton state go back and forth several times and run away from RC to some extent, allowing annihilation to happen until the irreversible-CS.

The significant annihilation in the dimer might reflect its ability to quench excess energy more efficiently than that of the monomer. The quenching is seemingly contradictory for efficient light-energy conversion. However, as in the cases of light-harvesting complex 1[37] and photosystem I,[38] antenna Chls and RC are often separated by a few tens of angstroms. These separations could protect the RC from damage caused by excess excitation. Actually, there are some reports that quenching excess energy in a thylakoid membrane, including PSII-CC, takes place at high light intensity.[39,40] Moreover, it

DOI: 10.1021/jacs.6b04316
J. Am. Chem. Soc. 2016, 138, 11599−11605

was recently reported that some Chls in PSII-CC could act as trap sites leading to the photoprotection.[16] Because the monomer can easily dimerize in the lipid-free conditions,[22] the dimerization under the strong light intensity might take an important role in the control of the light energy being transferred into RC.

MATERIALS AND METHODS

Preparation of PSII-CC. Monomeric and dimeric PSII-CC were separated and purified from the thermophilic cyanobacterium *Thermosynechococcus vulcanus* as described previously[18,41] in 30 mM 2-(*N*-morpholino)ethanesulfonic acid (MES) buffer containing 20 mM NaCl, 3 mM $CaCl_2$, 0.03% w/v *n*-dodecyl beta-D-maltoside, and 5% w/v glycerol. Monomeric PSII-CC was used for TA spectroscopy measurements after being purified by column chromatography. The quality of dimeric PSII-CC was further improved by recrystallization steps.[3,6,18] Then, the dimeric PSII-CC crystals were transferred into the buffer solution and used for TA spectroscopy measurements.

Transient Absorption Spectroscopy. The experimental setup for TA measurements is similar to those utilized in previous studies.[42,43] The femtosecond Ti:sapphire laser (Tsunami, Spectra-Physics) was pumped by the SHG of a cw Nd^{3+}:YVO_4 laser (Millennia V, Spectra-Physics). The output of the Ti:sapphire laser was regeneratively amplified with 1 kHz repetition rate (Spitfire, Spectra-Physics), and the amplified pulse had an energy of 1 mJ/pulse and pulse duration of 85 fs fwhm. The amplified pulse was divided into two pulses with a 50/50% beam splitter and guided into a pair of noncollinear optical parametric amplifier systems (TOPAS-white, Light-Conversion). The wavelength of the outputs of TOPAS-white were controlled by computers. The polarization between the pump and probe pulses was set at magic angle. The optical path of the sample cell was 1 mm, and the optical density of the sample was <0.8 at 676 nm as shown in Figure 1. A homemade rotating cell was used (2000 rpm) to avoid optical damage of the sample and accumulate long-lived species. The distance from the center of the rotating cell to the laser focusing point was ∼5 mm; thus, the length of periphery was ∼31 mm, and the rotation velocity was ∼1.0 m/sec. Assuming a focused spot size of ∼0.3 mm, it requires ∼100 shots before hitting the same position. The fluctuation of the individual laser pulse was observed by oscilloscope and was estimated to be less than 10%.

Self-diffraction frequency-resolved optical gating (SD-FROG) measurement was carried out to obtain the autocorrelation trace of the pump pulse. The pulse duration was optimized to be the shortest at the sample position by a pulse compressor inside TOPAS-white with two wedged, fused silica plates. The output of TOPAS-white with its spectrum centered at ∼640 nm was utilized to excite the PSII-CC. The pulse duration was ∼20 fs. Meanwhile, by focusing the output of the other TOPAS-white (center wavelength: 980 nm) into a rotating CaF_2 window (optical path: 2 mm), white-light supercontinuum was generated.

The signal and the reference pulses in the wavelength range of 400−900 nm were detected with two pairs of spectrometer and multichannel photodiode array system (PMA-10, Hamamatsu), and the data were sent to a personal computer for further analysis. A cross-correlation trace between the pump pulse and the white-light supercontinuum was obtained by an optical Kerr effect (OKE) measurement. A group velocity dispersion curve of the experimental setup was obtained by least-squares-fitting of the cross-correlation trace, and the TA signals were calibrated based on this data.

For the TA data to be analyzed, regression analysis was performed based on least-squares method utilizing data analysis software (Igor Pro 6, WaveMetrics), and the coefficient confidence intervals were set to 95% to estimate the errors (standard deviations) of the time constants.

ASSOCIATED CONTENT

Supporting Information

The Supporting Information is available free of charge on the ACS Publications website at DOI: 10.1021/jacs.6b04316.

TA data and details of estimation of the excitation laser fluence (PDF)

AUTHOR INFORMATION

Corresponding Author

*ynagasa@fc.ritsumei.ac.jp

Notes

The authors declare no competing financial interest.

ACKNOWLEDGMENTS

Y.N. was supported by Precursory Research for Embryonic Science and Technology (PRESTO), Japan Science and Technology Agency (JST). Y.Y. was supported by a fellowship from The Interactive Materials Science Cadet (IMSC) program. This work was also supported by JSPS KAKENHI Grant Number 26107002 in Scientific Research on Innovative Areas "Photosynergetics". The authors thank Prof. Shigeichi Kumazaki (Kyoto University) for helpful discussion and comments.

REFERENCES

(1) Shen, J.-R. *Annu. Rev. Plant Biol.* **2015**, *66*, 23−48.
(2) Vinyard, D. J.; Ananyev, G. M.; Charles Dismukes, G. *Annu. Rev. Biochem.* **2013**, *82*, 577−606.
(3) Umena, Y.; Kawakami, K.; Shen, J.-R.; Kamiya, N. *Nature* **2011**, *473*, 55−60.
(4) Suga, M.; Akita, F.; Hirata, K.; Ueno, G.; Murakami, H.; Nakajima, Y.; Shimizu, T.; Yamashita, K.; Yamamoto, M.; Ago, H.; Shen, J.-R. *Nature* **2015**, *517*, 99−103.
(5) Loll, B.; Kern, J.; Saenger, W.; Zouni, A.; Biesiadka, J. *Nature* **2005**, *438*, 1040−1044.
(6) Kamiya, N.; Shen, J.-R. *Proc. Natl. Acad. Sci. U. S. A.* **2003**, *100*, 98−103.
(7) Zouni, A.; Witt, H.-T.; Kern, J.; Fromme, P.; Krauss, N.; Saenger, W.; Orth, P. *Nature* **2001**, *409*, 739−743.
(8) Schatz, G. H.; Brock, H.; Holzwarth, A. R. *Proc. Natl. Acad. Sci. U. S. A.* **1987**, *84*, 8414−8418.
(9) Schatz, G. H.; Brock, H.; Holzwarth, A. R. *Biophys. J.* **1988**, *54*, 397−405.
(10) Vassiliev, S.; Orth, P.; Zouni, A.; Owens, T. G.; Bruce, D. *Proc. Natl. Acad. Sci. U. S. A.* **2001**, *98*, 8602−8607.
(11) Vassiliev, S.; Lee, C.-I.; Brudvig, G. W.; Bruce, D. *Biochemistry* **2002**, *41*, 12236−12243.
(12) Holzwarth, A. R.; Müller, M. G.; Reus, M.; Nowaczyk, M.; Sander, J.; Rögner, M. *Proc. Natl. Acad. Sci. U. S. A.* **2006**, *103*, 6895−6900.
(13) Raszewski, G.; Renger, T. *J. Am. Chem. Soc.* **2008**, *130*, 4431−4446.
(14) Mohamed, A.; Nagao, R.; Noguchi, T.; Fukumura, H.; Shibata, Y. *J. Phys. Chem. B* **2016**, *120*, 365−376.
(15) Hastings, G.; Durrant, J. R.; Barber, J.; Porter, G.; Klug, D. R. *Biochemistry* **1992**, *31*, 7638−7647.
(16) Shibata, Y.; Nishi, S.; Kawakami, K.; Shen, J.-R.; Renger, T. *J. Am. Chem. Soc.* **2013**, *135*, 6903−6914.
(17) Tumino, G.; Casazza, A. P.; Engelmann, E.; Garlaschi, F. M.; Zucchelli, G.; Jennings, R. C. *Biochemistry* **2008**, *47*, 10449−10457.
(18) Shen, J.-R.; Kamiya, N. *Biochemistry* **2000**, *39*, 14739−14744.
(19) Kern, J.; Loll, B.; Lüneberg, C.; DiFiore, D.; Biesiadka, J.; Irrgang, K. D.; Zouni, A. *Biochim. Biophys. Acta, Bioenerg.* **2005**, *1706*, 147−157.

DOI: 10.1021/jacs.6b04316
J. Am. Chem. Soc. 2016, 138, 11599−11605

(20) Kuhl, H.; Kruip, J.; Seidler, A.; Krieger-Liszkay, A.; Bünker, M.; Bald, D.; Scheidig, A. J.; Rögner, M. *J. Biol. Chem.* **2000**, *275*, 20652−20659.
(21) Watanabe, M.; Iwai, M.; Narikawa, R.; Ikeuchi, M. *Plant Cell Physiol.* **2009**, *50*, 1674−1680.
(22) Takahashi, T.; Inoue-Kashino, N.; Ozawa, S.; Takahashi, Y.; Kashino, Y.; Satoh, K. *J. Biol. Chem.* **2009**, *284*, 15598−15606.
(23) Broser, M.; Gabdulkhakov, A.; Kern, J.; Guskov, A.; Müh, F.; Saenger, W.; Zouni, A. *J. Biol. Chem.* **2010**, *285*, 26255−26262.
(24) Zimmermann, K.; Heck, M.; Frank, J.; Kern, J.; Vass, I.; Zouni, A. *Biochim. Biophys. Acta, Bioenerg.* **2006**, *1757*, 106−114.
(25) Holt, N. E.; Kennis, J. T. M.; Fleming, G. R. *J. Phys. Chem. B* **2004**, *108*, 19029−19035.
(26) Konermann, L.; Holzwarth, A. R. *Biochemistry* **1996**, *35*, 829−842.
(27) de Weerd, F. L.; van Stokkum, I. H. M.; van Amerongen, H.; Dekker, J. P.; van Grondelle, R. *Biophys. J.* **2002**, *82*, 1586−1597.
(28) Vacha, F.; Joseph, D. M.; Durrant, J. R.; Telfer, A.; Klug, D. R.; Porter, G.; Barber, J. *Proc. Natl. Acad. Sci. U. S. A.* **1995**, *92*, 2929−2933.
(29) Raszewski, G.; Saenger, W.; Renger, T. *Biophys. J.* **2005**, *88*, 986−998.
(30) Nuijs, A. M.; van Gorkom, H. J.; Plijter, J. J.; Duysens, L. N. M. *Biochim. Biophys. Acta, Bioenerg.* **1986**, *848*, 167−175.
(31) Trinkunas, G.; Herek, J. L.; Polívka, T.; Sundström, V.; Pullerits, T. *Phys. Rev. Lett.* **2001**, *86*, 4167−4170.
(32) Yoneda, Y.; Noji, T.; Katayama, T.; Mizutani, N.; Komori, D.; Nango, M.; Miyasaka, H.; Itoh, S.; Nagasawa, Y.; Dewa, T. *J. Am. Chem. Soc.* **2015**, *137*, 13121−13129.
(33) Bennett, D. I. G.; Amarnath, K.; Fleming, G. R. *J. Am. Chem. Soc.* **2013**, *135*, 9164−9173.
(34) Broess, K.; Trinkunas, G.; van der Weij-de Wit, C. D.; Dekker, J. P.; van Hoek, A.; van Amerongen, H. *Biophys. J.* **2006**, *91*, 3776−3786.
(35) Miloslavina, Y.; Szczepaniak, M.; Müller, M. G.; Sander, J.; Nowaczyk, M.; Rögner, M.; Holzwarth, A. R. *Biochemistry* **2006**, *45*, 2436−2442.
(36) Chmeliov, J.; Trinkunas, G.; van Amerongen, H.; Valkunas, L. *J. Am. Chem. Soc.* **2014**, *136*, 8963−8972.
(37) Hu, X.; Damjanović, A.; Ritz, T.; Schulten, K. *Proc. Natl. Acad. Sci. U. S. A.* **1998**, *95*, 5935−5941.
(38) Krauss, N.; Schubert, W.-D.; Klukas, O.; Fromme, P.; Witt, H. T.; Saenger, W. *Nat. Struct. Biol.* **1996**, *3*, 965−973.
(39) Holt, N. E.; Zigmantas, D.; Valkunas, L.; Li, X.-P.; Niyogi, K. K.; Fleming, G. R. *Science* **2005**, *307*, 433−436.
(40) Baker, N. R. *Annu. Rev. Plant Biol.* **2008**, *59*, 89−113.
(41) Shen, J. R.; Inoue, Y. *Biochemistry* **1993**, *32*, 1825−1832.
(42) Ishibashi, Y.; Katayama, T.; Saito, H.; Yamanaka, K.-i.; Goto, Y.; Tani, T.; Okada, T.; Inagaki, S.; Miyasaka, H. *J. Phys. Chem. C* **2014**, *118*, 9419−9428.
(43) Nagasawa, Y.; Fujita, K.; Katayama, T.; Ishibashi, Y.; Miyasaka, H.; Takabe, T.; Nagao, S.; Hirota, S. *Phys. Chem. Chem. Phys.* **2010**, *12*, 6067−6075.

DOI: 10.1021/jacs.6b04316
J. Am. Chem. Soc. 2016, 138, 11599−11605